

621.651:532.595

Paper No. 218-13

Study of a Piston Pump without Valves*

(1st Report, On a Pipe-capacity-system with a T-junction)

By Shoji TAKAGI**, Toru SAIJO***

This paper concerns a piston pump without valves which consists of a piping system with a T-junction, two water tanks connected with both ends of the main pipe and a piston installed in the lateral pipe. Pump effect occurring in the system is examined theoretically and experimentally. The study is confined to the case that the time average flow in the main pipe is zero. The pump effect is a phenomenon that part of the energy corresponding to the time averages of kinetic energy in both of the main pipe is stored in one side of the tanks. Influences of system parameters on the pumping effect were clarified. The results obtained from a mathematical model proposed in this paper were found to be in good agreement with the experimental data.

Key Words : Fluid Vibration, Unsteady Flow, Pump, Bio-Mechanics, T-Junction

1. Introduction

Piston pumps used for industrial purpose usually have directional control valves. On the other hand, G.Liebau has proposed several piston pumps without valves (i.e. ventillose Kolbenpumpe) in order to understand the phenomenon in the blood circulation systems, that is, the pumping effect of the heart of valvular disease⁽¹⁾⁻⁽³⁾. A representative model consists of two flexible tubes of different cross sectional areas and thicknesses connected together in series and an oscillating plate which forces the part of the flexible tube wall to move in the radial direction. The pump of this type is able to yield a head of a few meters. This pump has been modified by H.J.Bredow in such form that the part of a flexible tube with a uniform cross section is excited sinusoidally and two tanks with a considerably large cross sectional area are connected with both ends of the tube⁽⁴⁾. And he has investigated it experimentally and theoretically. O.Mahrenholtz has proposed a model of the blood circulation system with the heart of valvular disease which is composed of a closed loop main conduit of a T-junction (abbreviated to tee), a tank and a piston in the lateral pipe of the tee⁽⁵⁾. And he has clarified theoretically that the pumping effect can occur in the system. Except for the above mentioned studies related with physiology, T.Matsui has studied experimentally the flow in the main pipe of a tee both ends of which terminate in the tanks in the case that the oscillating flow is delivered in the lateral pipe, and clarified that the time-average flow occurs and the water level in the tank connected with the longer pipe is higher than the other if the system construction is asymmetric with respect to the tee (see Fig.1)⁽⁶⁾. As we have seen, there are a lot of studies

on the piston pumps without valves. However, the mechanism of the pumping effect and the factors which influence the phenomenon may have hardly clarified.

This paper discusses the mechanism of the pumping effect of a piston pump without valves which has a T-junction. The discussion is confined to the case that the time-average flow is zero (abbreviated to the case of zero discharge), because the essence of the phenomenon may be clarified most easily in this case.

2. Experimental Apparatus and Method

The arrangement of an experimental setup is schematically shown in Fig.1. The water tanks with a large cross sectional area (2500 cm²) are installed at both ends of the main pipe of the tee. The lateral pipe is connected with a cylinder through the nozzle C and a polyvinyl chloride resin pipe with inner diameter D (4 cm). The sinusoidal oscillating flow is delivered in the lateral pipe by use of the piston (with effective cross sectional area $A_p=28.27$ cm²) which is driven by a motor with a stepless speed change device through the scotch yoke

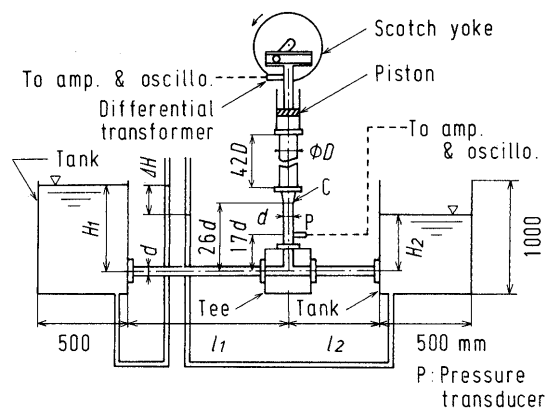


Fig.1 Schematic diagram of the experimental setup

* Received 6th April, 1981.

** Associate Professor, Department of Energy Engineering, Toyohashi Univ. of Technology, Toyohashi 440, Japan.

*** Engineer, Toyota Motor Co., Ltd., Toyota 471, Japan.

device. Figure 2 shows the dimensions of two tees, which are made of brass by machining, with a square sectional area used in the experiment. The only difference between tee No.1 and tee No.2 is the radius of curvature of the joining edge r . The main and the lateral pipes were composed of several pipes with the same cross section as the tee, each of which was made of transparent acrylic resin by machining. The piping system was installed on the same horizontal plane. The friction factors of the main and the lateral pipes were in good agreement with Blasius formula for turbulent flow.

The frequency of the piston f was varied in the range between 0.2 and 1.6 Hz. The difference between the water levels in both the tanks ΔH was measured by a manometer when the water in the main pipe was in a steady oscillating state, that is, the state that the time-average flow is zero. The judgement whether the oscillation is in a steady state or not was made by observing the motion of an air bubble of almost 1 cm³ which was put into "the longer pipe", which is one side of the tee from the tank is longer than the other side (hereafter to be called "the shorter pipe"). The amplitude of the oscillation of flow was obtained by measur-

ing the displacement of the air bubble. Considerable attention was paid to decrease the influence of the change of kinematic viscosity resulting from the change of the water temperature as much as possible, that is, we made water circulate sufficiently before measurement and reduced the time for measuring by setting the water level in each tank nearly in a steady state.

3. Experimental Results

First, we discussed the dimensionless parameters which govern the head ΔH by use of the dimensional analysis under the assumption that the shape and dimensions of the piping system and the tanks are constant. The following relation was obtained.

$$\Delta H/d = F(S_0, Re_0, G) \dots\dots\dots(1)$$

where $\Delta H = H_1 - H_2$, H_1 : head in the tank connected with the longer pipe (see Fig.1), H_2 : head in the other tank, $S_0 = d^3/A_p S$, $Re_0 = A_p S \omega / \nu$, $G = \omega^2 d / g$, d : side length of the square cross section of the pipe, A_p : effective cross sectional area of the piston, S : amplitude of the piston, ω : angular frequency, g : acceleration of gravity, F : a function. The parameter Re_0 represents the velocity amplitude in the lateral pipe, and S_0 corresponds to the amplitude of the piston S . The dimensionless frequency $\Omega = \omega d^2 / \nu$ is also used to represent characteristics of unsteady flow in pipes. The parameters Ω , Re_0 and S_0 can be related to $Re_0 = \Omega / S_0$, therefore $\Delta H/d$ can be also represented as a function of S_0 , Ω and G .

Figure 3(a) shows the measured $\Delta H/d$ against Re_0 for S_0 as parameter and Fig.3(b) for G . We can see from the figures that the influence of S_0 and G on $\Delta H/d$ may be considerably smaller than that of Re_0 . This fact means that the $\Delta H/d$ hardly depends on the amplitude and the frequency of the piston when the frequency is low enough. Therefore, $\Delta H/d$ will be plotted against Ω for several constant values of S_0 hereafter.

Examples of measured $\Delta H/d$ are shown in Fig.4. It can be seen that the head in the

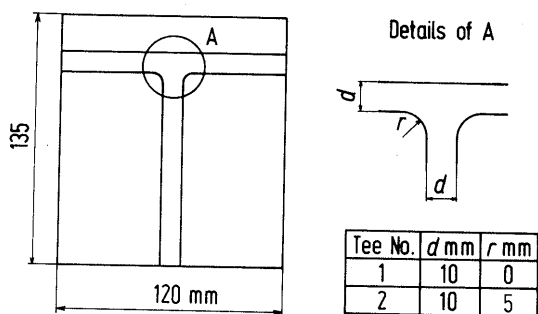
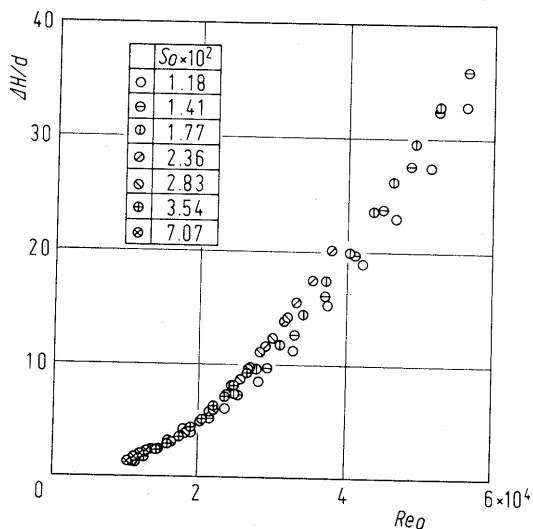
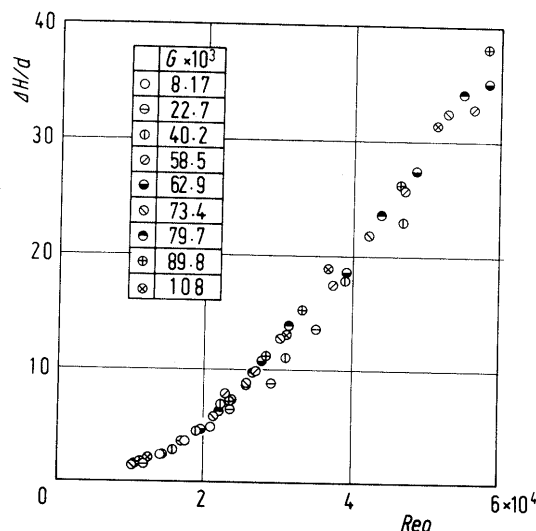


Fig.2 Dimensions of tees used



(a)



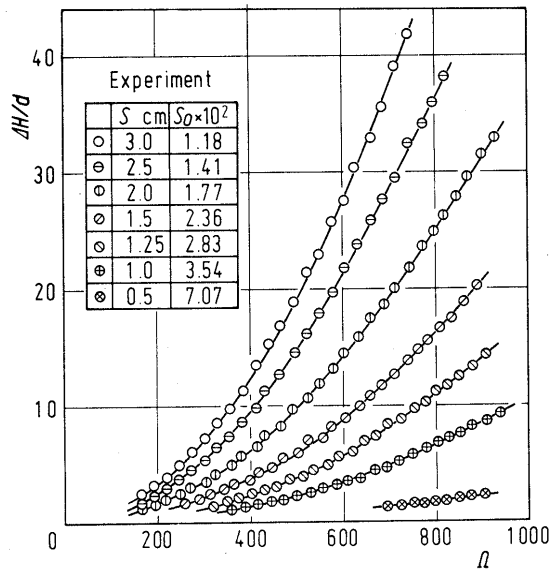
(b)

Tee No.1, $l_1=269$ cm, $l_2=29$ cm

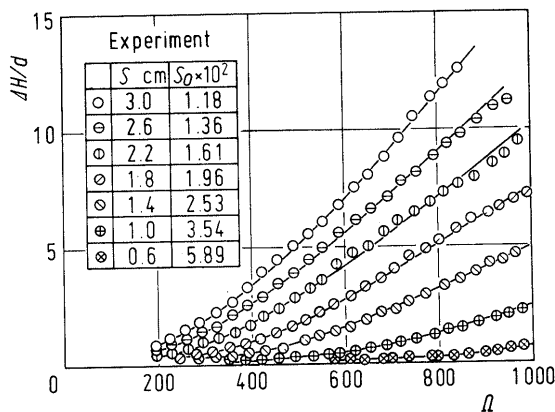
Fig.3 $\Delta H/d$ vs. Re_0 characteristics

tank connected with the longer pipe is always higher than the head in the other tank in the whole range of frequencies. And the head $\Delta H/d$ obtained by using tee No.1 with a sharp joining edge is several times as high as the one obtained by using tee No.2. Therefore, it can be stated that the flow characteristics of tees may have a great influence on the pumping effect of the system.

4. Mathematical Model and Discussion



(a) Tee No.1



(b) Tee No.2

$l_1=269$ cm, $l_2=29$ cm

Fig.4 Head in the case of zero discharge

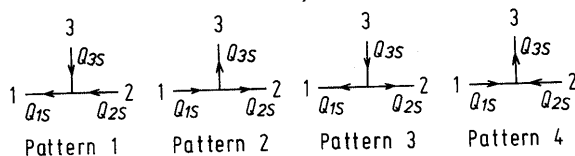


Fig.5 Flow patterns at tees

As mentioned above, the pumping effect may greatly depend on the flow in the vicinity of junctions. From the stand point of constructing a mathematical model which can predict the motion of the system, it may be necessary that the characteristics of the flow at tees be expressed in a reasonable form. Firstly we will discuss the steady state flow characteristics at tees.

4.1 Steady State Flow Characteristics at Tees

The energy losses caused by the combination and division of flow at smooth tees with circular cross section have been clarified for each of all flow patterns⁽⁷⁾. Although there have been several studies on the energy losses at tees with square cross section for the usual flow patterns⁽⁸⁾, there are hardly any reports on the flow patterns in which a fluid flows from both sides of the main pipe into the lateral pipe or flows from the lateral pipe into both sides of the main pipe so far as the authors are aware of.

Thinking that the motion in the main pipe should be considered, we adopted the energy equation between two sections, which are positioned in both sides of the main pipe, as the characteristics at tees. The flow patterns through a symmetrical tee are shown in Fig.5. It can be seen that there are four kinds of flows which differ fundamentally from each other. We call each of the flow "pattern n" hereafter, where n=1, 2,3,4. The magnitude of the volume discharge in the *i*th branch (where *i*=1,2,3) is denoted by Q_{is} as shown in Fig.5, and the flow direction by the arrow. The energy equation between the 1st and 2nd branches becomes

$$\frac{p_1}{\rho} + \frac{v_1^2}{2} + \lambda_1 \frac{L_1}{d} \frac{v_1^2}{2} \text{sgn } v_1 + g \Delta h_{12} \text{sgn } v_2 = \frac{p_2}{\rho} + \frac{v_2^2}{2} + \lambda_2 \frac{L_2}{d} \frac{v_2^2}{2} \text{sgn } v_2 \dots \dots \dots (2)$$

where p_i : pressure, v_i : mean velocity (whose positive direction is the direction denoted by the arrow in pattern 3 in Fig.5), $\Delta h_{12} [= \zeta_{12}(v_m^2/2g)]$: loss due to the division or combination of flow between sections 1 and 2, ζ_{12} : loss coefficient, $v_m = \max(|v_1|, |v_3|)$, L_i : length of the *i*th branch, λ_i : friction factor, ρ : density of fluid, sgn : sign function. The experimental results of the loss coefficient ζ_{12} are shown in Fig.6 for each flow pattern. The solid line denotes the experimental one for Reynolds number $Re=9000$, where $Re=v_m d/\nu$, the dot-dot-dash-line the one obtained by Sato⁽⁶⁾ and the brokenline the one for circular pipes by Ito and Imai⁽⁷⁾. The loss coefficients for tees No.1 and No.2 are very close to each other and are almost independent of Reynolds number larger than 9000 for patterns 2 and 4 in which the water in the lateral pipe flows away from the tee. On the other hand, there is a great difference between the coefficients for pattern 1 and for pattern 3, and ζ_{12} for tee No.2 depends remarkably on Reynolds number in the vicinity of the order of 10000. The dot-dash-line in pattern 3 for tee No.2 will be mentioned later.

4.2 Mathematical Model

A schematic diagram of the system under study is shown in Fig.7, in which Q_0 is the amplitude of the volume flow in the lateral pipe, ω the angular frequency, t the time, P_i and P_{ti} the pressures at the position indicated in the figure where $i=1,2$, Q_i the volume flow in the main pipe, P_{ci} the pressure at the tank ends, S_i the cross sectional area of the tank, H_i the water level in the tank, A the cross sectional area of the pipe, and l_i the length of the pipe. We can derive basic equations of the system on the basis of the following assumptions: (i) The working fluid is incompressible. (ii) S_i is so large that the oscillation of the water level in the tanks can be neglected. (iii) The law of pipe friction and flow characteristics at the tee are steady state ones. (iv) The loss due to division or combination of flow at the tee occurs in the region indicated in Fig.7 by the broken line.

The continuity equation and the momentum equation are

$$Q_1 + Q_2 = Q_0 \cos \omega t \quad \dots\dots\dots(3)$$

$$m_i \dot{Q}_i + 4(l_i/d)\tau_i \operatorname{sgn} Q_i = P_i - P_{ci} \quad (i=1, 2) \quad \dots\dots\dots(4)$$

where $m_i = \rho l_i A / A$, τ_i is the wall shearing stress averaged over the pipe periphery, a dot denotes differentiation with respect to t . The wall shearing stress is

$$\tau_i = (\rho/8A^2)\lambda_i Q_i^2 \quad \dots\dots\dots(5)$$

where λ_i is the friction factor and is given as follows⁽⁹⁾⁻⁽¹¹⁾

For laminar flow

$$\lambda_i = 56.88 / (|Q_i|/vd) \quad \dots\dots\dots(6)$$

For turbulent flow

$$\lambda_i = 0.3164 / (|Q_i|/vd)^{0.25} \quad \dots\dots\dots(7)$$

Blasius formula was adopted for turbulent flow. The relation between the pressure in the tank and the water level is

$$P_{ci} = \rho g H_i \quad \dots\dots\dots(8)$$

At the tank ends of the main pipe the following equation holds.

$$P_{ci} = \begin{cases} P_i & (Q_i \geq 0) \\ P_i - (\rho/2A^2)(1 + \zeta_i)Q_i^2 & (Q_i < 0) \end{cases} \quad \dots\dots\dots(9)$$

where ζ_t is the loss coefficient for the flow from the tanks to the pipes. Taking account of the symmetry of the tee and the assumption (iii), we can represent the flow characteristics at the tee as follows

$$P_1 - P_2 = (\rho/2A^2)(Q_1^2 - Q_2^2 \mp \zeta_{12} Q_1 Q_2 \operatorname{sgn} Q_2) \quad \dots\dots\dots(10)$$

where $Q_3 = Q_1 + Q_2$, $Q_m = \max\{|Q_1|, |Q_2|, |Q_3|\}$, ζ_{12} is a function of the flow ratio $|Q_j/Q_k|$ ($j, k=1, 2; |Q_k| > |Q_j|, j \neq k$) and the upper sign of the double sign corresponds to the case of $|Q_1| > |Q_2|$ and the lower one to $|Q_1| < |Q_2|$.

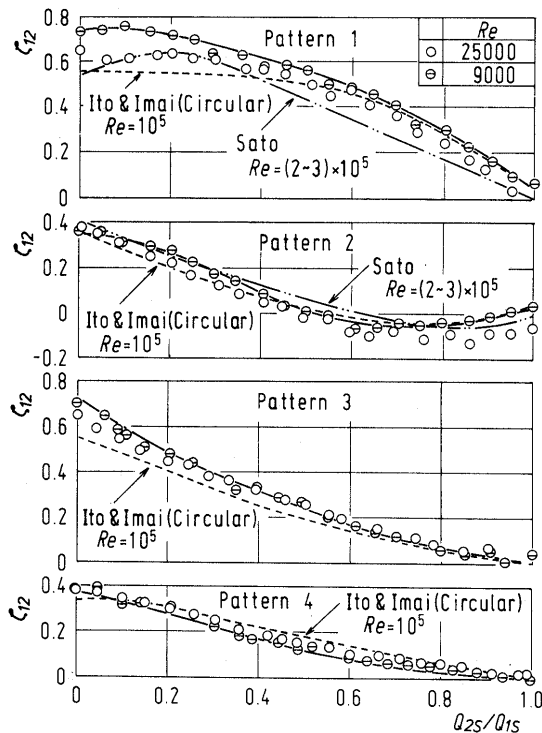
Equations (3)~(10) are the basic equations of the system. These equation can be reduced to

$$\left. \begin{aligned} (m_1 + m_2)\dot{Q}_1 + (\rho/2A^2)\{(1 + \zeta_1 - \zeta_{c1})Q_1^2 - (1 + \zeta_2 - \zeta_{c2})Q_2^2 \pm \zeta_{12} Q_1 Q_2 \operatorname{sgn} Q_2\} \\ = -m_2 Q_2 \omega \sin \omega t - \rho g \Delta H, \\ Q_2 = Q_0 \cos \omega t - Q_1, \quad Q_3 = Q_1 + Q_2 \end{aligned} \right\} \quad \dots\dots\dots(11)$$

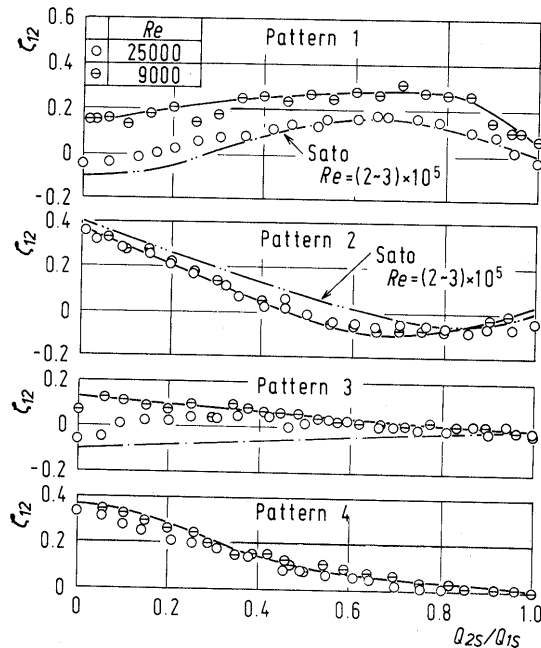
where $\zeta_i = (l_i/d)\lambda_i \operatorname{sgn} Q_i$, ζ_{ti} is zero when $Q_i > 0$ and $1 + \zeta_t$ when $Q_i < 0$.

4.3 Discussion

Equation (11) is a nonlinear first



(a) Tee No.1



(b) Tee No.2

Fig.6 Coefficients of head loss at tees

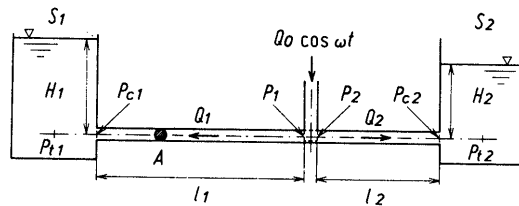


Fig.7 Schematic diagram of the system under study

order differential equation with time varying coefficients, and so it may be impossible to solve Eq.(11) in general. Consequently we analyzed Eq.(11) approximately in order to discuss qualitatively the head obtained from the system and examined in detail by numerical approach.

4.3.1 Characteristics in the Case of Zero Discharge

In this subsection the head in the case of zero discharge is discussed under the assumption that the flow rates Q_1 and Q_2 vary in the same phase. Then the expression of Q_1 or Q_2 is

$$Q_i = Q_{i0} \sin(\omega t + \delta) \quad (i=1, 2) \dots\dots\dots(12)$$

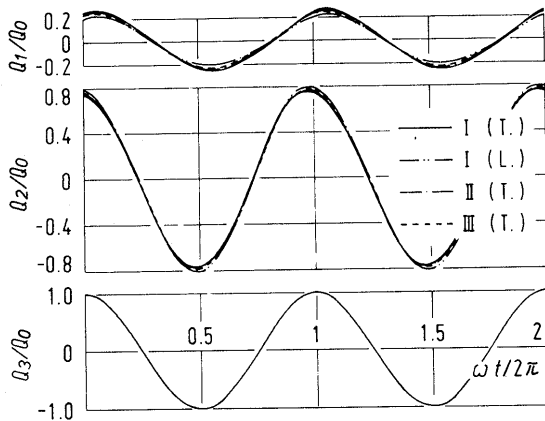
where Q_{i0} and δ are constants. Assuming $Q_{10} < Q_{20}$, the difference between the heads in both of the tanks ΔH is obtained by substituting Eq.(12) into Eqs.(4)(9)(10) and averaging both sides of these equations with respect to the time. We have

$$\Delta H = H_1 - H_2 = (1/8A^2g) \{ (Q_{10}^2 - Q_{20}^2) + (\eta_3 - \eta_4)(Q_{10} + Q_{20})^2 - \zeta_1(Q_{10}^2 - Q_{20}^2) \} \dots\dots\dots(13)$$

where η_3 is ζ_{12} for pattern 3, and η_4 for pattern 4. After examining Eq.(13), we can obtain the following conclusions: (i) Pumping effect can occur in the system even if the head loss due to division or combination of flow and the entrance head loss at the tank can be neglected. In this case, the water level in one side of the tanks, which

Table 1 Loss coefficient ζ_{12} used for numerical computation

No.	Loss coefficient ζ_{12}
I	The solid line in Fig.6(a) (Tee No.1, $Re=9000$)
II	The solid line in Fig.6(b) (Tee No.2, $Re=9000$)
II'	Pattern 1,2,4 : The same as II Pattern 3 : The dot-dash-line in Fig.6(b)
III	$\zeta_{12}=0$



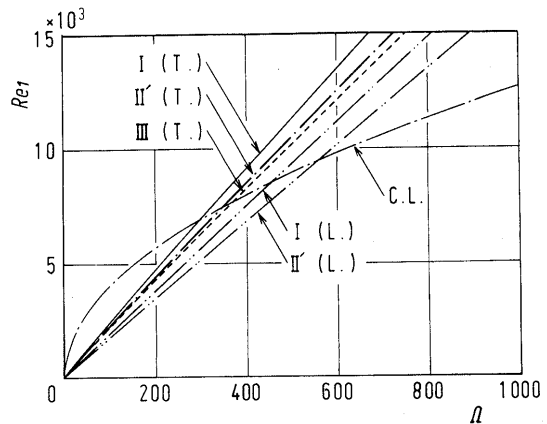
$l_1=244$ cm, $l_2=54$ cm, $d=1$ cm,
 $S_0=1.18 \times 10^{-2}$, $\Omega=500$

Fig.8 Several examples of computed waveforms

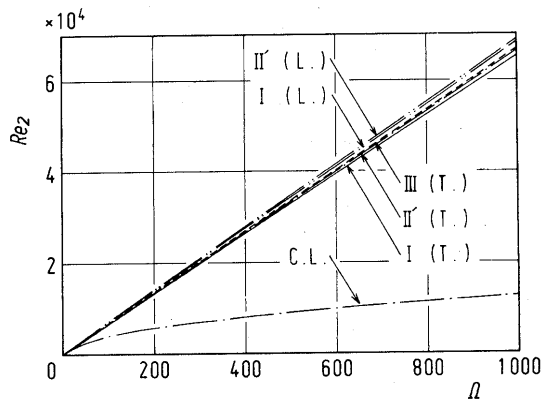
is connected with the pipe having a smaller flow amplitude, is higher than the other side. And the difference of the water level increases in proportion to an increase in the difference between the amplitude of flows. This means that when the time average of kinetic energy in one side of the main pipe is not equal to the one in the other side, part of the difference is stored as potential energy in one side of the tanks connected with the pipe having smaller kinetic energy. (ii) The head loss for pattern 3 helps increase ΔH , but the one for pattern 4 helps decrease it. (iii) The entrance loss at one side of the tanks which has a smaller amplitude of flow helps increase ΔH , but the one at the other side helps decrease it. (iv) The head loss due to wall friction does not appear explicitly in Eq.(13), but it has an influence on ΔH as the factor determining Q_{10} and Q_{20} .

4.3.2 Results from Numerical Approach and Consideration

In this subsection we discuss the results on the characteristics in the case of zero discharge obtained by integrating Eq.(11) numerically by use of a digital computer. In the computation, we used four kinds of loss coefficients at the tee shown in Table 1 and two friction factors of Eq.(6) and Eq.(7).



(a) Re_1 vs. Ω curves

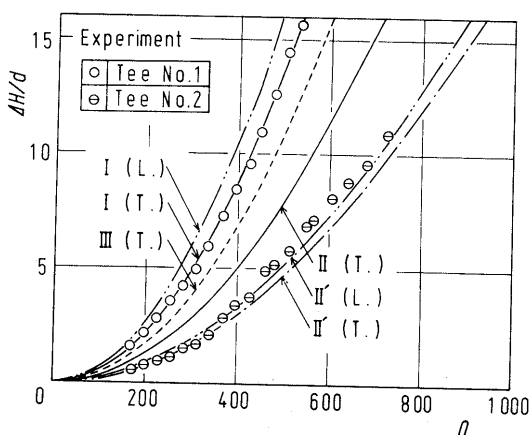


(b) Re_2 vs. Ω curves

$l_1=244$ cm, $l_2=54$ cm, $d=1$ cm, $S_0=0.0118$

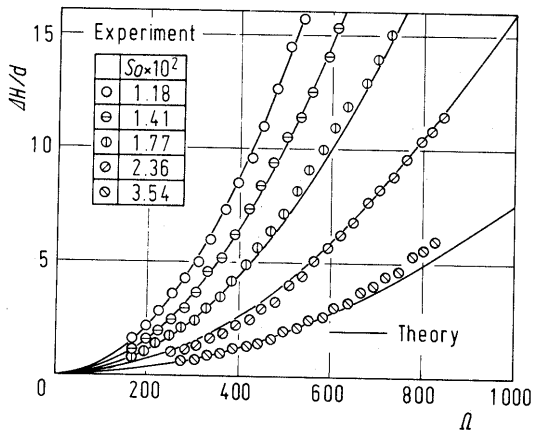
Fig.9 Calculated dimensionless amplitudes of velocity

Several computed waveforms of the main flow discharges Q_1 and Q_2 are shown with the flow discharge in the lateral pipe $Q_3 = Q_0 \cos \omega t$ in Fig.8. The line indicated with symbol I, II or III was obtained by using the loss coefficient corresponding to the same symbol in Table 1. The symbol (L.) corresponds to the friction factor for laminar flow [see Eq.(6)] and (T.) for turbulent flow [see Eq.(7)]. These symbol will be used in the same meaning hereafter. It is

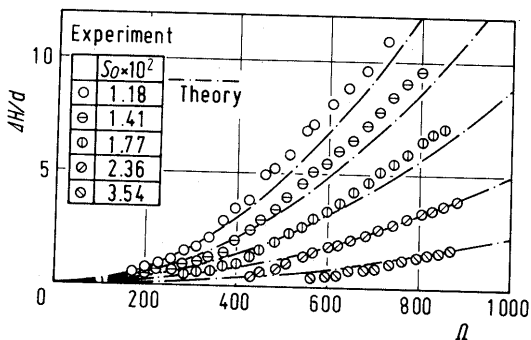


$l_1=244$ cm, $l_2=54$ cm, $d=1$ cm, $S_0=0.0118$

Fig.10 Comparison of the experimental data with the calculated curves



(a) Tee No.1



(b) Tee No.2

$l_1=244$ cm, $l_2=54$ cm, $d=1$ cm

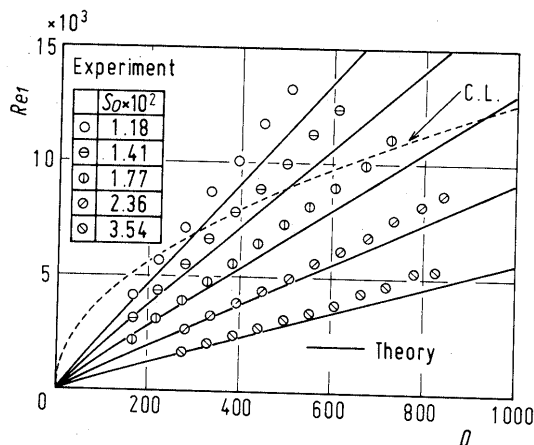
Fig.11 Characteristics in the case of zero discharge

seen from Fig.8 that the waveforms of Q_1 and Q_2 hardly change even when configuration of pipe friction is changed. The flows Q_1 and Q_2 vary in almost the same phase and these fundamental components are predominant. This may prove validity of the prerequisite for the analysis in subsection 4.3.1.

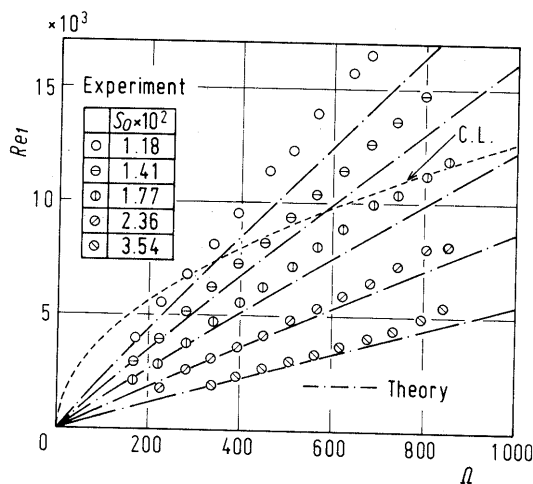
In Fig.9 are shown calculated lines of the dimensionless amplitude of flow in the main pipe Re_1 and Re_2 , where Re_i ($i=1,2$) is

$$Re_i = U_i d / \nu \dots\dots\dots (14)$$

in which U_i is the amplitude of flow in the main pipe. When the ratio l_1/l_2 is considerably large such as the case shown in Fig. 9, the amplitude of flow in the shorter pipe is as large as several times the one in the longer pipe and hardly depends on the loss coefficient at the tee and on the configuration of pipe friction. The dot-dash-line C.L. has the following meaning: It has been clarified for unsteady flow in circular pipes with diameter d that when Re_i exceeds the critical Reynolds number Re_c defined by Eq.(15), instantaneous velocity distributions for almost all phases in one cycle of oscillation obey Blasius's power formula and friction factors



(a) Tee No.1



(b) Tee No.2

$l_1=244$ cm, $l_2=54$ cm, $d=1$ cm

Fig.12 Measured amplitudes of velocity and calculated curves

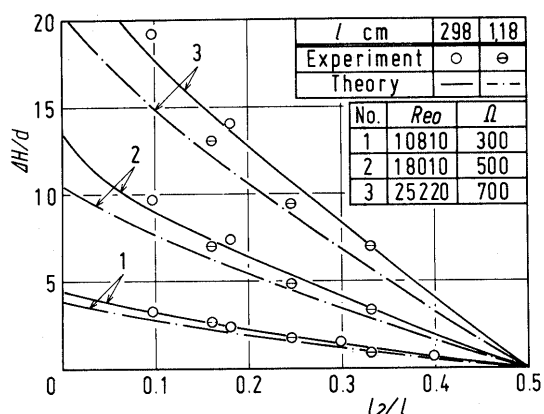


Fig.13 Heads against pipe length ratio

are in good agreement with Blasius's formula⁽¹¹⁾

$$R_{ec} = 400\sqrt{\Omega} \dots \dots \dots (15)$$

The line C.L. in Fig.9 represents Eq.(15).

Figure 10 shows the calculated lines and the measured values of ΔH against Ω . We can see that the measured values for tee No.1 are in good agreement with the theoretically predicted line I(T.). However, there are some discrepancies between the line II(T.) and the measured values for tee No.2. The discrepancies may be understood as follows: The loss coefficients ζ_{12} of tee No.2 for flow patterns 1 and 3 depends considerably on Reynolds number in the vicinity of $Re=9000$ (see Fig.6). The coefficient ζ_{12} measured for $Re=9000$ may not represent sufficiently the actual coefficient in operation when $Re_0 [= \Omega/S_0] > 10^4$ in which the experiment was made. So we modified ζ_{12} of II in Table 1 in the form that ζ_{12} for pattern 3 is only replaced with the dot-dash-line in Fig.6(b), and using this modified coefficient (i.e. II' in Table 1), we obtained the calculated line II'(T.). The line II'(T.) is in good agreement with the measured values. The broken line in Fig.10 is a calculated one when the head of loss at the tee is neglected. The head ΔH in this case is a little lower than the one for tee No.1 but rather higher than the one for tee No.2. This is caused by the fact that for tee No.1 ζ_{12} for pattern 3 is larger than the one for pattern 4, while for tee No.2 the reverse is true. This result conforms well to the analytical conclusion (ii) stated in subsection 4.3.1. It is also seen that the configuration hardly affects ΔH when $l_1 \gg l_2$. Taking account of the above mentioned results, we will show the calculated results on the head ΔH obtained by using the loss coefficients ζ_{12} of I and II' in Table 1 and the friction factor for turbulent flow hereafter.

Experimental and theoretical ΔH vs. Ω characteristics are shown for S_0 as parameter in Fig.11. The measured values are in good agreement with the theoretically predicted ones. Figure 12 shows dimensionless

amplitudes in the longer pipe Re_l under the same operational condition as the above. The experimental values were obtained from measured amplitudes of displacement of the fluid in the longer pipe under the assumption that the fluid oscillates sinusoidally. The line C.L. indicates Eq.(15). It is seen from Fig.11 and Fig.12 that the mathematical model proposed in this paper may represent well the pumping effect of the system.

The head ΔH for tee No.1 is shown in Fig.13 against pipe length ratio l_2/l where $l (=l_1+l_2)$ is total length of the main pipe. The head ΔH depends a little on the total length for the identical operating condition and for the identical pipe length ratio.

5. Conclusions

The pumping effect of a piston pump without valves, which is constructed of a piping system with a T-junction and a piston, is studied theoretically and experimentally. The results are summarized as follows:

- (1) The pumping effect occurring in this type of systems is a phenomenon that when the difference between the amplitudes of flow velocity in the main pipe connected with both sides of the junction occurs, pressure energy corresponding to the difference between the time averages of kinetic energy in both sides of the main pipe and to the energy loss at the junction and at the ends of the main pipe is stored in one side of the tanks connected with both ends of the main pipe.
- (2) Influences of system parameters on the pumping effect were clarified.
- (3) A mathematical model proposed in this paper can predict well the pumping effect of the system.

The authors wish to express their gratitude to Prof. Tadaya Ito, Nagoya Univ., for valuable discussion.

References

- (1) Liebau, G., Z. ges. exp. Medizin, 123-1(1954), 71.
- (2) Liebau, G., Naturwiss., 41-14(1954), 327.
- (3) Liebau, G., Z. ges. exp. Medizin, 125-5(1955), 483.
- (4) Bredow, H.J., Fortschr.-Ber., VDI-Z, 7-9(1968).
- (5) Mahrenholtz, O., Forsch. Ing.-wess., 29-2(1963), 47.
- (6) Matui, T., et al., Preprint of JSME (Suwa) (in Japanese), (1966-10), 85.
- (7) Ito, H. and Imai, K., Proc. Amer. Soc. Civ. Engr., 99-HY9, (1973-9), 1353.
- (8) Sato, Y., Trans. JSME (in Japanese), 28-192, (1962), 881.
- (9) Ohmi, M. and Iguchi, M., Trans. JSME (in Japanese), 46-404, B(1980-4), 628.
- (10) Ohmi, M., et al., Trans. JSME (in Japanese), 46-405, B(1980-5), 846.
- (11) Ohmi, M. and Iguchi, M., Trans. JSME (in Japanese), 47-418, B(1981-6), 993.